Received: 16 July 2021 | Revised: 10 August 2021 | Accepted: 12 August 2021

DOI: 10.1002/jmr.2933

RESEARCH ARTICLE

Journal of Molecular Recognition WILEY

Comparison on binding interactions of quercetin and its metal complexes with calf thymus DNA by spectroscopic techniques and viscosity measurement

Huajian Luo[1] | Yu Liang[1] | Huiying Zhang[2] | Yi Liu[1,3] | Qi Xiao[1] | Shan Huang[1]

[1]Guangxi Key Laboratory of Natural Polymer Chemistry and Physics, College of Chemistry and Materials, Nanning Normal University, Nanning, China

[2]College of Chemistry and Biological Engineering, Hechi University, Hechi, China

[3]State Key Laboratory of Separation Membranes and Membrane Processes, School of Chemistry and Chemical Engineering, Tiangong University, Tianjin, China

Correspondence
Qi Xiao and Shan Huang, Guangxi Key Laboratory of Natural Polymer Chemistry and Physics, College of Chemistry and Materials, Nanning Normal University, Nanning 530001, China.
Email: qi.xiao@whu.edu.cn (Q. X.) and huangs@nnnu.edu.cn (S. H.)

Funding information
National Natural Science Foundation of China, Grant/Award Numbers: 21763005, 21563006, 21864006, 21563010; Natural Science Foundation of Guangxi Province, Grant/Award Numbers: 2017GXNSFDA198034, 2017GXNSFFA198005, 2021GXNSFAA075015; BAGUI Scholar Program of Guangxi Province of China; Thousands of Young Teachers Training Program of Guangxi Province, Grant/Award Number: guijiaoren[2018]18

Abstract

Quercetin (Qu) and its metal complexes have received great attention during the last years, due to their good antioxidant, antibacterial, and anticancer activities. In this contribution, binding interactions of Qu and Qu–metal complexes with calf thymus DNA (ctDNA) were investigated and compared systematically by using spectroscopic techniques and viscosity measurement. UV-vis absorption spectra of ctDNA–compound systems showed obvious hypochromic effect. Relative viscosity and melting temperature of ctDNA increased after the addition of Qu and Qu–metal complexes, and the change tendency is Qu–Cr(III) > Qu–Mn(II) > Qu–Zn(II) > Qu–Cu(II) > Qu. Fluorescence competition experiments show that hydrogen bonds and van der Waals interaction play an important role in the intercalative binding of Qu and Qu–metal complexes with ctDNA. Qu and Qu–metal complexes could unwind the right-handed B-form helicity of ctDNA and further affect its base pair stacking. Space steric hindrance might be responsible for the differences in the intercalative binding between ctDNA and different Qu–metal complexes. These results provide new information for the molecular understanding of binding interactions of Qu–metal complexes with DNA and the strategy for research of structural influences.

KEYWORDS
calf thymus DNA, chiral conformation, intercalative binding, metal complexes, quercetin

1 | INTRODUCTION

Quercetin (Qu), which is one of the most abundant natural flavonoids and polyphenolic compounds presented in various vegetables and fruits, is one of the primary active components of plentiful natural Chinese traditional medicines.[1-3] Many researches have indicated that Qu is equipped with a broad pharmacological activity, such as anticancer, antiviral, antibacterial, antioxidant, and anti-inflammatory effects.[4,5] Since Qu can scavenge reactive oxygen species (ROS) including •OH, H_2O_2 and O^{2-} efficiently, it can protect DNA from damage induced by ROS either as a free molecular species or at a site where it binds to DNA.[6,7] In recent years, various metal cations can chelate with Qu to form stable Qu–metal complexes, which have attracted great interest by biochemists and biomedical scientists due to their better antioxidant, antibacterial, and anticancer activity.[8,9] For example, Qu–Cu(II) complex can prevent the production of ROS and exhibits higher antioxidant activity in comparison with pure Qu.[10] Qu–Cu(II) and Qu–Zn(II) complexes exhibited superior antitumor

Huajian Luo and Yu Liang contributed equally to this work.

activities to Qu alone.[11] Qu–Ni(II) complex showed antitumor activity which might be related to its intercalation into DNA structure and DNA-binding selectivity.[12] These results demonstrate that the combination of Qu and metal ions is a promising starting point for the development of novel Qu-based antioxidant and anticancer drugs.

DNA, which plays a major role during the replication and transcription of genetic information of life process, is one of the main targeted biomacromolecules of several anticancer drugs.[13] Investigation of binding interactions between DNA and important anticancer drugs have become an active and important subject in many research fields, since such researches can provide valuable information for the development of effective target anticancer therapeutic agents.[14-16] Binding interactions of Qu and its metal complexes with DNA have been extensively studied, as their unusual binding properties, combined with their general photochemical properties, make them appropriate probes for DNA secondary structure, conformation, photocleavers, and antitumor drugs.[17,18] Tan et al investigated the DNA binding and oxidative DNA damage induced by Qu–Cu (II) complex.[19] Ni et al researched the interaction between Qu–Cu (II) complex and DNA by using a neutral red dye fluorescent probe.[20] Hu and coworkers have systematically studied the structure-activity relationship of Qu and naringenin with DNA.[21] Collectively, these findings give an understanding of the structure-activity relationships which may be helpful in the design of analogs of these flavonoids and their application in drug and food industries.

It is well-known that the binding modes between small molecules and DNA are mainly electrostatic attraction, groove binding, and intercalative binding.[7,22] Among three binding modes, intercalative binding can lead to the unwinding and the lengthening of the DNA helix.[23] Although some small molecules can intercalate with DNA bases, detailed influencing factors are quite complicated and kinetic mechanisms of their interactions are still unrevealed. Systematical investigation of binding modes and interaction mechanisms between small molecules and DNA are very significant to the research of conformation variation of DNA and the directional design of efficient anticancer drugs against several diseases. Although the interactions between some Qu–metal complexes and calf thymus DNA (ctDNA) have been reported previously, the systematical investigation and comparison of the interactions among these Qu–metal complexes with ctDNA are still unrevealed clearly. Inspired by these facts, we investigated and compared the binding interactions of Qu and Qu–metal complexes with ctDNA by viscosity measurements, DNA melting, and spectroscopic techniques in this work. This study will be helpful to the development of novel flavonoid based therapeutic agents that target DNA for severe diseases and to the development of antioxidants that can be used in drug and food industries.

2 | EXPERIMENTAL

2.1 | Reagents

Qu and ctDNA were purchased from Sigma-Aldrich (St. Louis, MO, USA). $ZnSO_4$, $MnSO_4{\cdot}H_2O$, $CuCl_2{\cdot}2H_2O$, and $CrCl_3{\cdot}6H_2O$ were purchased from Sinopharm Chemical Reagent Factory Co. Ltd. (Shanghai, China). The stock solution of Qu (3.0×10^{-3} mol L^{-1}) was prepared by dissolving its crystals in ethyl alcohol. The ctDNA was dissolved in Tris-HCl buffer (pH 7.4) and stored in refrigerator. The concentration of ctDNA was determined spectrophotometrically using an extinction coefficient at 260 nm of 6600 L mol^{-1} cm^{-1}.[24] The purity of ctDNA was verified by monitoring the ratio of absorbance at 260 and 280 nm. All other chemical reagents were of analytical reagent grade. Ultrapure water was used throughout the whole experiment.

2.2 | Apparatus

UV-vis absorption spectra were measured on Cary 100 UV-vis spectrophotometer (Agilent Technologies, Inc., Australia). Fluorescence spectra were performed on RF-5301 PC luminescence spectrometer (Shimadzu Co., Ltd., Tokyo, Japan). Circular dichroism (CD) spectra were recorded on Chirascan CD spectrometer (Applied Photophysics, England). Viscosity measurements were carried out using a viscosity meter (Yinhua Flowmeter Co. Ltd., China). All pH measurements were made with a basic pH meter PB-10 (Sartorius Scientific Instruments Co., Ltd., China).

2.3 | Procedures

2.3.1 | Preparation of Qu–metal complexes

Qu–metal complexes were prepared according to the literature method.[19] Solid Qu (3.0×10^{-3} mol L^{-1}) was dissolved in 60 mL of ethanol. The pH of solution was adjusted to around 7.0. After 5 minutes, different metal ion solution with same concentration (1.5×10^{-3} mol L^{-1}) was added to the mixture. The mixture was stirred and heated to reflux for 5 hours at 50°C, and then the mixture was poured into H_2O. The brown-yellow precipitate was set aside for 48 hours, filtered, and washed three times with ethanol/H_2O solution (volume ratio of 1:3). The solid product was dried under a vacuum for 48 hours at room temperature. The possible structure models of Qu–metal complexes were shown in Figure 1.

2.3.2 | Viscosity measurements

Viscosity of ctDNA with different concentration of ethidium bromide (EB), acridine orange (AO), Qu, and Qu–metal complexes were measured in a viscometer that was kept at a constant temperature of 25 ± 0.1°C in a thermostatic water bath. Flow time measurements were performed by a digital stopwatch with a resolution of 0.001 second. At least five-time records reproducible to 0.02 second were obtained, and the average value was used in the calculations. Data were presented as $(\eta/\eta_0)^{1/3}$ vs [compound]/[ctDNA] value,[25] where η and η_0 were the viscosity values of ctDNA in the presence and absence of compound, respectively. Viscosity value was calculated from the

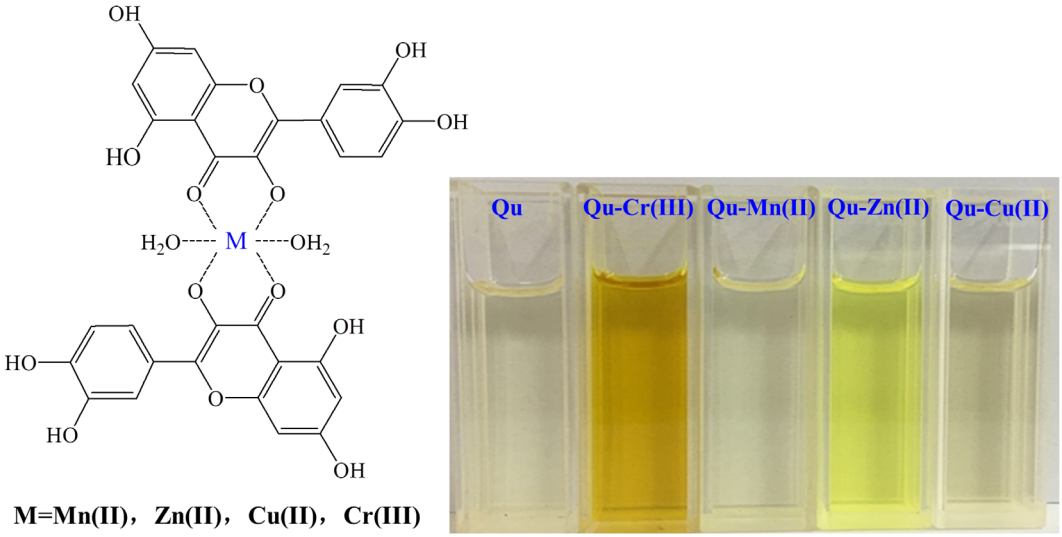

FIGURE 1 Structure models and solution colors of Qu–metal complexes

observed flow time of ctDNA containing solutions (t > 100 s) corrected for the flow time of buffer alone (t_0), $\eta = (t - t_0)/t_0$.

2.3.3 | DNA melting studies

DNA melting experiments were carried out by monitoring the absorbance of ctDNA at 260 nm in the absence and presence of compounds at different temperatures. The temperature was continuously monitored with a thermostatic bath. The absorbance was then plotted as a function of temperature ranging from 30°C to 95°C. The melting temperature of ctDNA was determined as the transition midpoint.

2.3.4 | Fluorescence spectra measurements

Fluorescence spectra of ctDNA–AO system at the presence of compounds were recorded at 298, 304, and 310 K with the excitation/emission slits of 3.0/3.0 nm. The excitation wavelength was 475 nm and the fluorescence intensity at 533 nm was recorded. The appropriate blanks corresponding to buffer were subtracted to correct the background of fluorescence. Titrations were performed manually by using trace syringes and each spectrum was the average of three scans.

2.3.5 | CD spectra measurements

CD spectra of ctDNA, compounds, and ctDNA-compound systems with different molar ratio of [compound]/[ctDNA] in Tris-HCl buffer (pH 7.4) were recorded from 220 to 320 nm at 25°C under constant nitrogen airflow. CD profiles were obtained using scan speed of 500 nm min^{-1} and response time of 0.5 second. Each spectrum was the average of three successive scans and was corrected by the buffer solution. Appropriate baseline corrections in CD spectra were made.

3 | RESULTS AND DISCUSSION

3.1 | UV-vis absorption spectrometry

UV-vis absorption spectra of ctDNA and compounds with different concentration of ctDNA in Tris-HCl buffer (pH 7.4) were shown in Figure 2. Due to the strong absorption of purine and pyrimidine bases, ctDNA shows a characteristic and maximum absorption peak of 260 nm.[26] Meanwhile, Qu, Qu–Cr(III), Qu–Mn(II), and Qu–Zn(II) complexes exhibit two absorption peaks at 267 and 376 nm (Figure 2A-D), respectively. However, Qu–Cu(II) complex shows an obvious absorption peak at 330 nm (Figure 2E). As inserted in Figure 2A-D, with the continuous addition of ctDNA, the absorbances of Qu, Qu–Cr(III), Qu–Mn(II), and Qu–Zn(II) complexes at 376 nm are decreased gradually, suggesting that ctDNA interacts with these compounds and subsequently affects their absorption characteristics. Usually, hyperchromic and hypochromic effects are regarded as the spectral characteristics of DNA-compound interactions, and hypochromic effect usually originates from the intercalative binding of small molecules with DNA double helical structure.[27,28] As shown in Figure 3A, obvious hypochromic effects exists at 376 nm after the interactions of ctDNA with Qu, Qu–Cr(III), Qu–Mn(II), and Qu–Zn(II) complexes. So Qu and these Qu–Cu(II) complex may interact with ctDNA through electrostatic forces, indicating that the interaction modes of ctDNA with these compounds may be the intercalative binding. Further shown in Figures 2E and 3A, the absorbance of Qu–Cu(II) complex at 330 nm increases slightly at lower concentration of ctDNA but decreases weakly at higher concentration of ctDNA. These results suggest that Qu–Cu(II) complex may interact with ctDNA at its lower concentration through electrostatic forces but intercalate into the double helical structure of ctDNA with higher concentration.[19]

In order to compare the interactions between ctDNA and these compounds, the quantity of hypochromism value (H) was obtained by the equation of $H = (A_{Free} - A_{Bounded})/A_{Free} \times 100\%$.[29] Herein, A_{Free} means the absorbances of Qu, Qu–Cr(III), Qu–Mn(II), and Qu–Zn

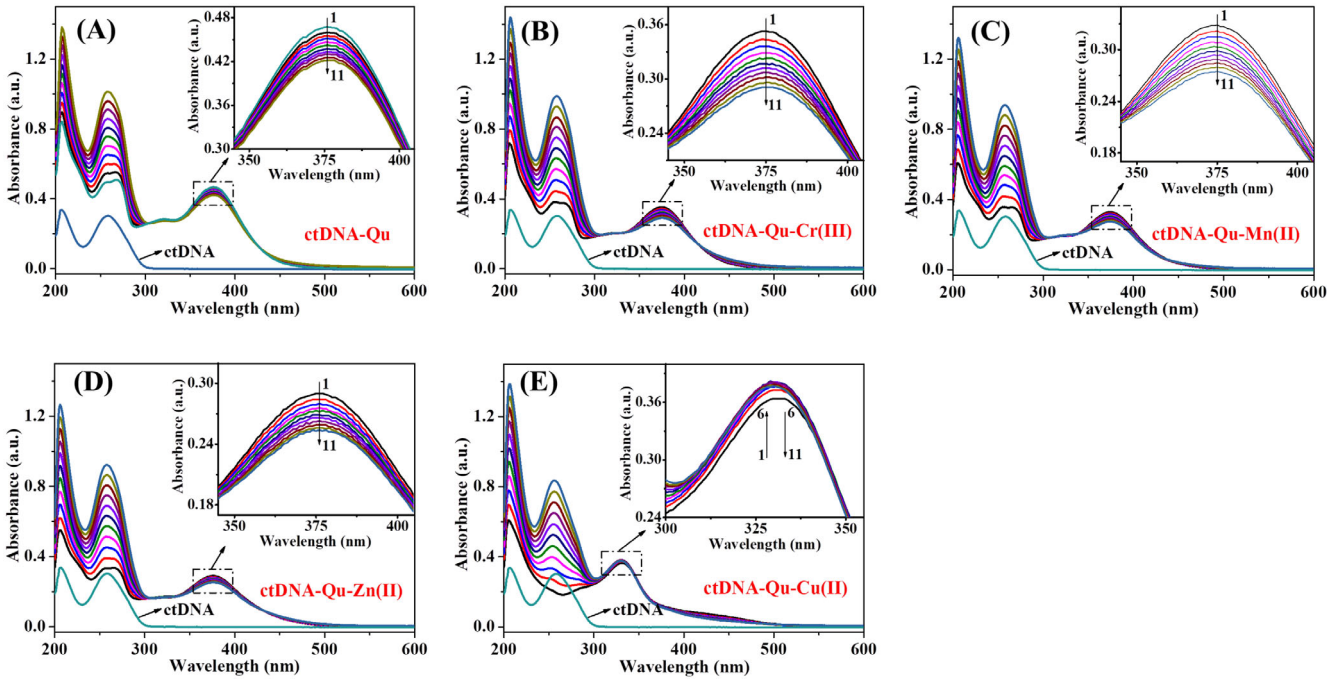

FIGURE 2 UV-vis absorption spectra of ctDNA and Qu (A), Qu-Cr(III) complex (B), Qu-Mn(II) complex (C), Qu-Zn(II) complex (D), and Qu-Cu (II) complex (E) with different concentration of ctDNA in Tris-HCl buffer (pH 7.4) at 25 oC. Inset: UV-vis absorption spectra of ctDNA with or without compounds in the wavelength range of 345 to 410 nm

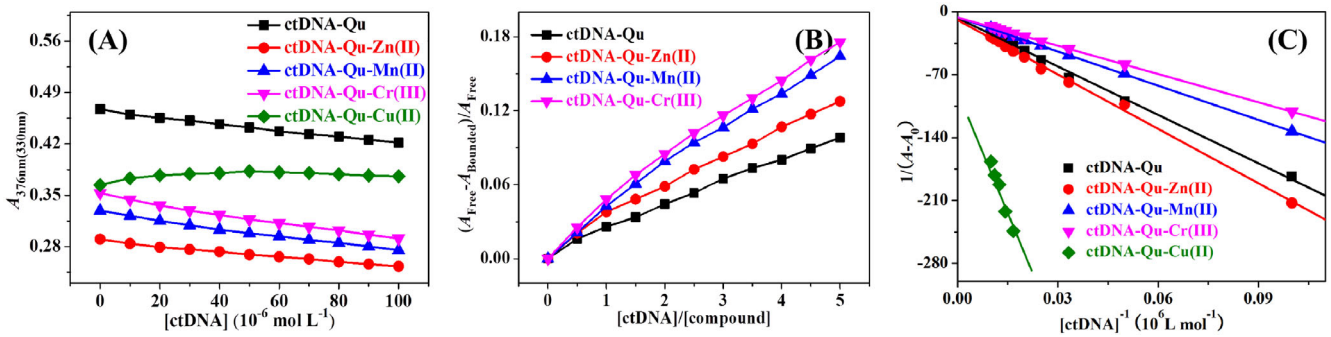

FIGURE 3 A, Plots of absorbance vs [ctDNA]. The absorbance at 376 nm for Qu, Qu-Cr(III), Qu-Mn(II), and Qu-Zn(II) complexes, while at 330 nm for Qu-Cu(II) complex. B, Curves of the quantity of hypochromism values vs [ctDNA]/[compound]. C, Plots of $1/(A-A_0)$ vs 1/[ctDNA]

(II) complexes at 376 nm or the absorbance of Qu–Cu(II) complex at 330 nm, while $A_{Bounded}$ is the absorbance of these compounds after the addition of ctDNA. As shown in Figure 3B, the hypochromism values of Qu, Qu–Cr(III), Qu–Mn(II), and Qu–Zn(II) complexes are all decreased with the increase of the concentration of ctDNA. Upon the addition of 1.0×10^{-4} mol L^{-1} ctDNA, the hypochromism values of these compounds from higher to lower are: 17.6% of Qu–Cr(III) complex, 16.4% of Qu–Mn(II) complex, 12.8% of Qu–Zn(II) complex, and 9.8% of Qu, respectively. Since the higher hypochromism value often reflects the stronger intercalative binding ability between DNA and small molecules, Qu–Cr(III), Qu–Mn(II), and Qu–Zn(II) complexes show stronger binding ability with ctDNA than Qu alone. Therefore, the addition of metal ions into Qu can enhance its binding ability with ctDNA to different extent. In comparison, Qu–Cr(III) complex can bind with ctDNA more tightly than the other two Qu–metal complexes. Comparably, a very small hypochromic effect of 1.6% is occurred in Qu–Cu(II) complex after the addition of 1.0×10^{-4} mol L^{-1} ctDNA, so Qu–Cu(II) complex can only intercalate with the double helical structure of ctDNA with high concentration, which is agreed well with the reported results.[9,19]

To quantitatively compare the intercalative binding ability of these compounds with ctDNA, the intrinsic binding constant (K_b) of compounds with ctDNA can be determined by using the following equation:[29,30]

$$\frac{1}{A-A_0}=\frac{1}{A_\infty-A_0}+\frac{1}{K_b(A_\infty-A_0)}\frac{1}{[\text{ctDNA}]} \quad (1)$$

Herein, A_0 and A are the absorbances of compound in the absence and presence of ctDNA, and A_∞ is the final absorbance of

ctDNA-compound system, respectively. The absorption peaks of Qu, Qu–Cr(III), Qu–Mn(II), and Qu–Zn(II) complexes are chosen at 376 nm, but the absorption peak of Qu–Cu(II) complex is chosen at 330 nm. In double reciprocal plots of $1/(A-A_0)$ vs $1/[\text{ctDNA}]$, the K_b value can be given by the ratio of the slope to the intercept. According to the plots in Figure 3C, the K_b values are calculated to be 6.23×10^3 L mol^{-1} for ctDNA–Qu–Cr(III) system, 4.98×10^3 L mol^{-1} for ctDNA–Qu–Mn(II) system, 4.64×10^3 L mol^{-1} for ctDNA–Qu–Zn(II) system, 4.18×10^3 L mol^{-1} for ctDNA–Qu–Cu(II) system and 4.01×10^3 L mol^{-1} for ctDNA–Qu system, respectively. The larger binding constant of ctDNA–Qu–Cr(III) system indicates that Qu–Cr(III) complex binds with the adjacent ctDNA double helical structure more tightly than other compounds. On the other hand, the binding constant of ctDNA–Qu system is the smallest, suggesting the weakest binding capability of Qu with ctDNA among these compounds. It can be speculated that the addition of metal ions can enhance the coplanarity of Qu–metal complexes, therefore these complexes can intercalate into the double helical structure of ctDNA mainly throng the π - π stacking interactions, thus resulting in the stronger binding strength with ctDNA.[9] Since Cr(III) possesses a higher electronic charge and less ionic radius, Qu–Cr(III) complex shows better stability and more coplanarity. Thus, among these Qu–metal complexes, Qu–Cr(III) complex exhibits the strongest intercalative binding interaction with ctDNA. This speculation will be further supported from other experiments investigated later, which gives convincing evidence of the possible intercalative binding between ctDNA and these compounds.

3.2 | Viscosity investigation

Viscosity experiment is an effective strategy to clarify the binding mode of DNA with small molecules. Usually, classical intercalative binding of small molecules with DNA base pairs causes the elongation of DNA and the increment of DNA viscosity significantly, while a partial or non-classical intercalative binding often causes a tiny change in the viscosity of DNA.[31] The influences of these compounds on the relative viscosity of ctDNA were shown in Figure 4A. It is obvious that the relative viscosity of ctDNA is increased gradually upon the continuous addition of these compounds, indicating that the interaction modes between ctDNA and these compounds may be the classic intercalative binding.[32] The detailed viscosity can be measured accurately by the slope value of the linear plot of $(\eta/\eta_0)^{1/3}$ vs [compound]/[ctDNA] (from 0 to 0.12).[22] As continuously shown in Figure 4B, the slope values are 0.995 for ctDNA–EB system, 0.940 for ctDNA–AO system, 0.924 for ctDNA–Qu–Cr(III) system, 0.889 for ctDNA–Qu–Mn(II) system, 0.872 for ctDNA–Qu–Zn(II) system, 0.846 for ctDNA–Qu–Cu(II) system and 0.777 for ctDNA–Qu system, respectively. However, the increase in viscosity of ctDNA for these compounds is lower than that for EB and AO. Usually, the slope value near 1.0 means an ideal intercalative binding,[33,34] so EB and AO are widely used intercalative probes in DNA. Since the slope values of these ctDNA–Qu–metal systems are relatively high, so Qu and Qu–metal complexes indeed intercalate into the base pairs of ctDNA and then increase the overall double helix length of ctDNA. The relative viscosity of ctDNA is increased steadily upon the addition of increasing concentrations of these compounds in the following order: Qu–Cr(III) > Qu–Mn(II) > Qu–Zn(II) > Qu–Cu(II) > Qu, showing that Qu–Cr(III) complex can intercalate with ctDNA more strongly and deeply than other compounds. These phenomena are highly consistent with the results obtained by UV-vis absorption spectrometry.

3.3 | DNA melting analysis

DNA melting analysis can be used for further elucidating the intercalative binding of small molecules and DNA. DNA melting temperature (T_m), which is the temperature at which half of duplex DNA denatured into two single strands, is dependent on the strength and the mode of its interaction with small molecules.[35,36] Intercalative binding of small molecules with DNA can stabilize the natural double helical structure of DNA and thus increase its T_m value obviously,

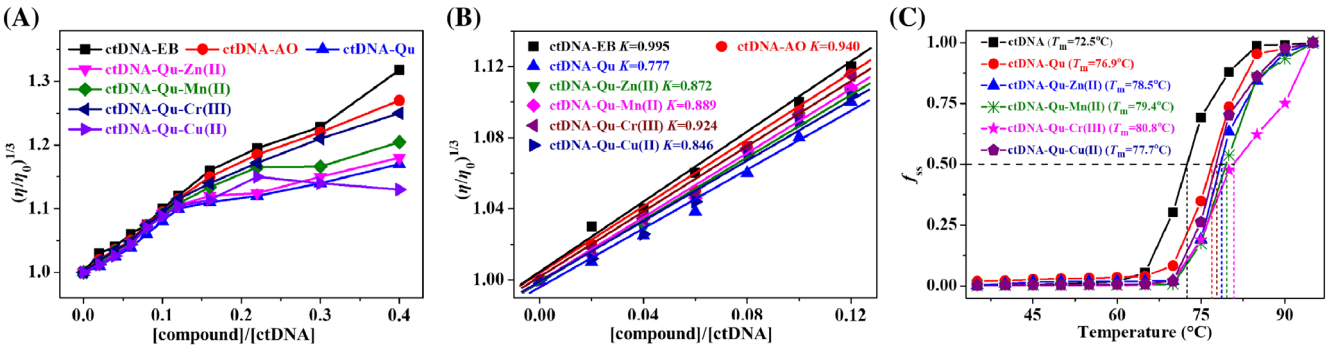

FIGURE 4 A, Curves of relative viscosity of ctDNA vs [compound]/[ctDNA]. c(ctDNA) = 5.0×10^{-5} mol L^{-1}; c(AO) = c(EB) = c(compound)/(10^{-6} mol L^{-1}): 0, 1, 2, 3, 4, 5, 6, 8, 11, 15, and 20. B, Plots of relative viscosity of ctDNA vs [compound]/[ctDNA]. c(ctDNA) = 5.0×10^{-5} mol L^{-1}; c(AO) = c(EB) = c(compound)/(10^{-6} mol L^{-1}): 0, 1, 2, 3, 4, 5, and 6. C, Melting curves of ctDNA in the absence and presence of these compounds. c(ctDNA) = 2.0×10^{-4} mol L^{-1}; c(compound) = 3.0×10^{-5} mol L^{-1}

while the electrostatic attraction and groove binding cause no distinct variation in the T_m value of DNA.[35,36] In order to clarify the interaction mechanism of these compounds with ctDNA, we recorded the absorbance of ctDNA at 260 nm in the absence and presence of compounds at different temperature with the temperature increasing gradually from 30°C to 95°C. Hence, the T_m value of ctDNA was obtained from the transition midpoint of the melting curves based on the relative absorbance (f_{ss}) vs temperature. Herein, $f_{ss} = (A\text{-}A_0)/(A_f\text{-}A_0)$, where A_0 is the initial absorbance of ctDNA-compound system, A is the absorbance of ctDNA-compound system corresponding to the temperature and A_f is the final absorbance of ctDNA-compound system, respectively.

As represented in Figure 4C, the T_m value of ctDNA alone is 72.5°C. After the addition of these compounds, the T_m value of ctDNA is increased to 80.8°C for ctDNA–Qu–Cr(III) system, 79.4°C for ctDNA–Qu–Mn(II) system, 78.5°C for ctDNA–Qu–Zn(II) system, 77.7°C for ctDNA–Qu–Cu(II) system and 76.9°C for ctDNA–Qu system, respectively. It is reported that the intercalative binding of natural or synthetic compounds into DNA often result in the increase of T_m value of about 5°C to 8°C, but the non-intercalative binding generally causes no significant increase of the T_m value.[36] These results further reveal the intercalative binding of these compounds with ctDNA. More interestingly, the T_m value of ctDNA is increased steadily upon the addition of these compounds in the following order: Qu–Cr(III) > Qu–Mn(II) > Qu–Zn(II) > Qu–Cu(II) > Qu, reconfirming the strongest intercalative binding ability of Qu–Cr(III) complex with ctDNA among these compounds.

3.4 | Fluorescence spectrometry

3.4.1 | Interaction modes

Interaction modes between DNA and small molecules can be elucidated by using the competitive fluorescence approach. The endogenous fluorescence of DNA is too weak, but some classic intercalating molecules can emit intense fluorescence in the presence of duplex DNA through strong stacking interactions.[37] Fluorescence of DNA–probe system can be efficiently quenched after the addition of other molecules by replacing the probe, and the extent of the fluorescence quenching of DNA–probe system can be used to clarify the detail interaction mode between small molecules and DNA.[22,37] Herein, the classic DNA intercalating molecule AO was chosen as the fluorescent probe. As indicated in Figure 5A-E, the fluorescence of AO is increased after its intercalative binding with ctDNA. The fluorescence of ctDNA(AO) system is decreased gradually after the addition of these compounds with increasing concentration. In addition, the fluorescence of ctDNA(AO) system is decreased linearly with the increasing concentration of compounds (inserts in Figure 5A-E), suggesting the intercalative binding of these compounds with ctDNA. Such experiments imply that these compounds can intercalate into the double helical structure of ctDNA and compete with AO for the intercalative site of ctDNA.

In order to compare the intercalative binding ability between ctDNA and these compounds, the fluorescence quenching effects were obtained by the equation of $Q = (I_0 - I)/I_0 \times 100\%$. Herein, I_0

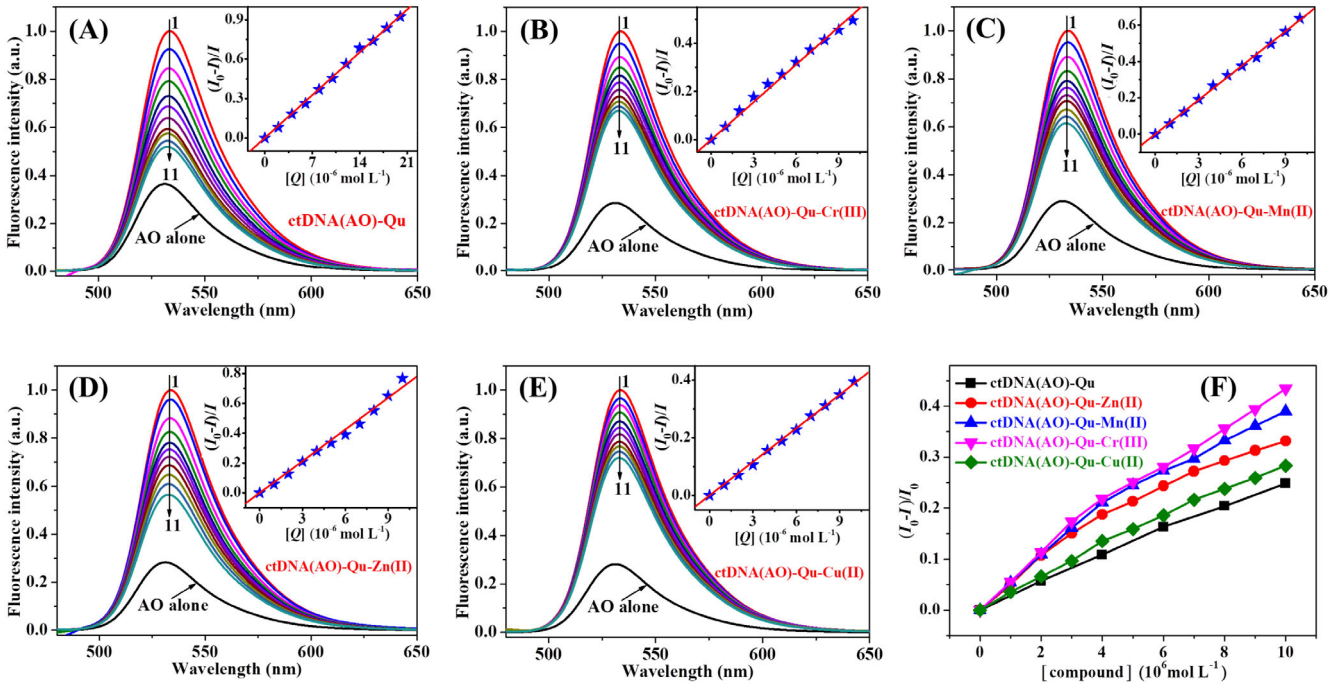

FIGURE 5 A-E, Fluorescence spectra of ctDNA(AO) system with various concentration of compounds. Inserts correspond to the Stern–Volmer plots. c(ctDNA) = 1.0 × 10^{-4} mol L^{-1}; c(AO) = 1.2 × 10^{-6} mol L^{-1}; c(Qu)/(10^{-6} mol L^{-1}), 1-11: from 0 to 20.0 at increments of 2.0; c (Qu metal complexes)/(10^{-6} mol L^{-1}), 1-11: from 0 to 10.0 at increments of 1.0. F, Curves of the fluorescence quenching values vs [compound]

and I are the fluorescence intensity of ctDNA(AO) system without or with these compounds, respectively. As shown in Figure 5F, the fluorescence quenching effects of ctDNA(AO) system are all increased with the increase of the concentration of these compounds. The results suggest that these compounds can substitute for some AO molecules and partial AO molecules dissociates from ctDNA(AO) complex into the solution. Upon the addition of 1.0×10^{-5} mol L^{-1} compounds, the fluorescence quenching effects of ctDNA(AO) system are 43.3% for Qu–Cr(III) complex, 38.3% for Qu–Mn(II) complex, 33.5% for Qu–Zn(II) complex, 28.6% for Qu–Cu(II) complex, and 23.5% for Qu, respectively. Since the higher fluorescence quenching effect often reflects the stronger intercalative binding ability between DNA and small molecules,[21] Qu–Cr(III) complex bind with ctDNA more tightly and replace AO molecules more efficiently than other compounds.

3.4.2 | Binding constants

Binding constants between these compounds and ctDNA can be calculated according to the fluorescence quenching plots of ctDNA(AO) complex after the addition of these compounds (inserts in Figure 5A-E). The fluorescence quenching of ctDNA(AO) complex by these compounds is in good agreement with the classical Stern–Volmer equation:[38]

$$\frac{I_0}{I} = 1 + K_{SV}[Q] \quad (2)$$

Herein, K_{SV} is the Stern–Volmer quenching constant and [Q] is the concentration of compound, respectively. So, the K_{SV} value can be determined by linear regression plot of I_0/I vs [Q]. Since these compounds can intercalate into the duplex ctDNA, the fluorescence quenching mechanism of these systems should be the static fluorescence quenching mode. In order to confirm the fluorescence quenching mechanism, the fluorescence spectra of ctDNA(AO) complex with different concentration of compounds were measured at three different temperatures (298, 304 and 310 K) and the fluorescence quenching data were all plotted by Stern–Volmer equation. As shown in Figure 6, the results agree well with the Stern–Volmer equation, which indicates that only either static or dynamic fluorescence quenching process is occurred. The calculated Stern–Volmer quenching constants K_{SV} values at three different temperatures were listed in Table 1. For ctDNA(AO)–Qu system, the K_{SV} values at three different temperatures are 4.65×10^4 L mol^{-1} at 298 K, 3.05×10^4 L mol^{-1} at 304 K and 2.25×10^4 L mol^{-1} at 310 K, respectively. For ctDNA(AO)–Qu–Cr(III) system, the K_{SV} values at three different temperatures are 5.19×10^4 L mol^{-1} at 298 K, 4.39×10^4 L mol^{-1} at 304 K and 3.64×10^4 L mol^{-1} at 310 K, respectively. It is very clear that the increase of the temperature results in the decrease of the K_{SV} values in all these systems. Quenching constant will be decreased with the increment of temperature for the static quenching process while the reverse is true for dynamic quenching process,[38] so the fluorescence quenching mechanism between these compounds and ctDNA(AO) complex is static fluorescence quenching.

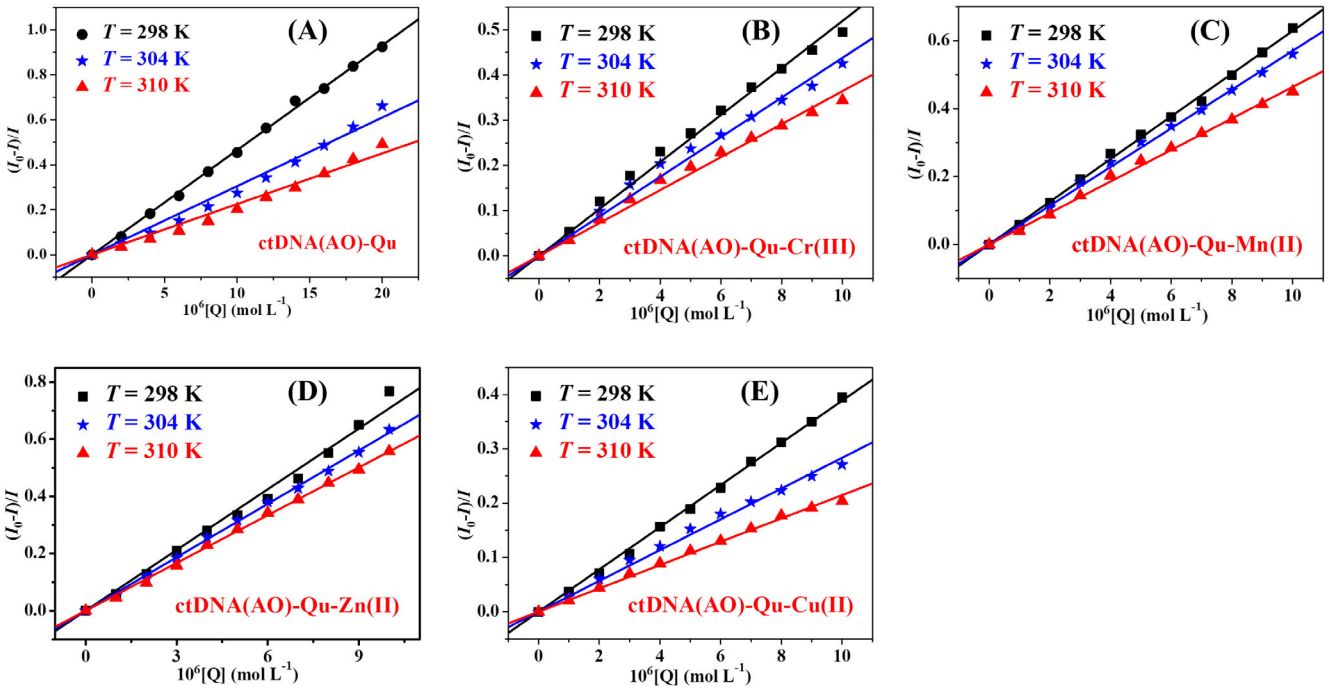

FIGURE 6 Stern–Volmer plots of ctDNA(AO)–Qu system (A), ctDNA(AO)-Qu-Cr(III) system (B), ctDNA(AO)-Qu-Mn(II) system (C), ctDNA(AO)-Qu-Zn(II) system (D), and ctDNA(AO)-Qu-Cu(II) system (E)

TABLE 1 Stern–Volmer quenching constants K_{SV}, associative binding constants K_a and relative thermodynamic parameters for the interactions between these compounds and ctDNA(AO) complex at three different temperatures

System	T (K)	K_{SV} (10^4 L mol^{-1})	R^{2a}	K_a (10^4 L mol^{-1})	R^{2a}	ΔH (kJ mol^{-1})	ΔG (kJ mol^{-1})	ΔS (J mol^{-1} K^{-1})	R^{2a}
ctDNA(AO)–Qu	298	4.65	0.999	2.70	0.998	−96.51	−25.25	−239.1	0.999
	304	3.05	0.997	1.21	0.999		−23.82		
	310	2.25	0.996	0.59	0.999		−22.38		
ctDNA(AO)–Qu–Zn(II)	298	7.08	0.995	2.92	0.998	−66.20	−25.58	−136.28	0.998
	304	6.23	0.999	1.97	0.997		−24.77		
	310	5.57	0.999	1.04	0.998		−23.95		
ctDNA(AO)–Qu–Mn(II)	298	6.29	0.999	3.67	0.998	−133.05	−26.01	−359.22	0.999
	304	5.71	0.998	1.22	0.998		−23.85		
	310	4.64	0.998	0.46	0.997		−21.69		
ctDNA(AO)–Qu–Cr(III)	298	5.19	0.997	5.03	0.997	−69.83	−26.78	−144.47	0.998
	304	4.39	0.995	2.73	0.995		−25.91		
	310	3.64	0.995	1.69	0.996		−25.04		
ctDNA(AO)–Qu–Cu(II)	298	3.88	0.999	2.85	0.999	−80.74	−25.50	−185.36	0.997
	304	2.83	0.999	1.66	0.998		−24.38		
	310	2.15	0.999	0.81	0.998		−23.27		

[a]R^2 is the correlation coefficient.

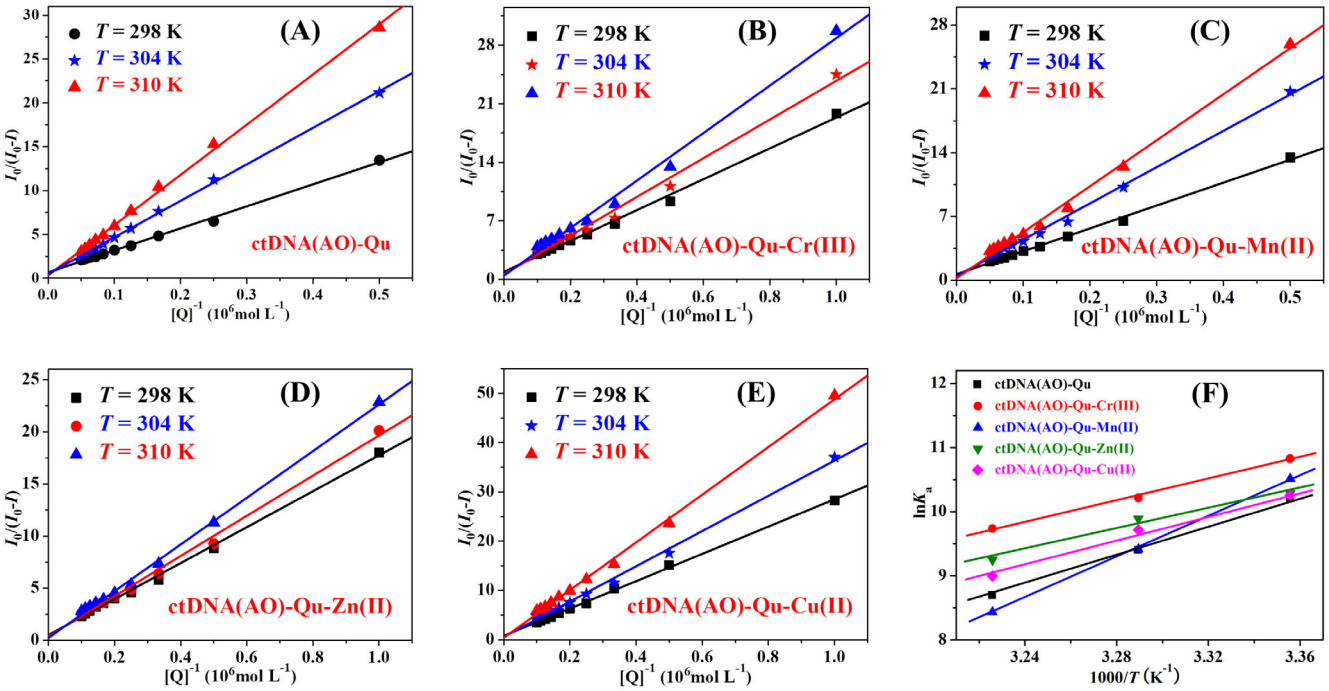

FIGURE 7 A-E, Modified Stern–Volmer plots of ctDNA(AO)–compound systems. F, Van't Hoff plots of ctDNA(AO)–compound systems

For static fluorescence quenching process, the associative binding constants (K_a) can be calculated through the modified Stern–Volmer equation[38]:

$$\frac{I_0}{I_0 - I} = \frac{I_0}{\Delta I} = \frac{1}{f_a K_a [Q]} + \frac{1}{f_a} \quad (3)$$

Herein, f_a is the mole fraction of solvent accessible fluorophore. So, the associative binding constant K_a value can be calculated from the quotient of the ordinate f_a^{-1} and the slope $(f_a K_a)^{-1}$. The modified Stern–Volmer plots were shown in Figure 7A-E, and the corresponding associative binding constants K_a were also listed in Table 1. The decreasing trend of K_a values with increasing

temperature is in accord with K_{SV}'s dependence on temperature, which reconfirms that the fluorescence quenching mechanism of ctDNA(AO) complex by these compound has mainly arisen from static fluorescence quenching mode. At the reaction temperature of 298 K, the K_a values of ctDNA(AO)–compound systems are 5.03×10^4 L mol^{-1} for ctDNA(AO)–Qu–Cr(III) system, 3.67×10^4 L mol^{-1} for ctDNA(AO)–Qu–Mn(II) system, 2.92×10^4 L mol^{-1} for ctDNA(AO)–Qu–Zn (II) system, 2.85×10^4 L mol^{-1} for ctDNA(AO)–Qu–Cu(II) system and 2.70×10^4 L mol^{-1} for ctDNA(AO)–Qu system, respectively. More interestingly, the K_a value of ctDNA(AO)–compound systems is increased steadily upon the addition of these compounds in the following order: Qu–Cr(III) > Qu–Mn(II) > Qu–Zn(II) > Qu–Cu(II) > Qu. The largest binding constant of ctDNA(AO)–Qu–Cr(III) system indicates that Qu–Cr(III) complex can intercalative with the duplex ctDNA most tightly, which is highly consistent with the above results.

3.4.3 | Binding forces

Binding forces contributing to DNA interactions with small molecules usually include hydrophobic forces, hydrogen bonds, electrostatic interactions and van der Waals interactions.[39] In general, binding forces can be elucidated by the variation of some thermodynamic parameters, such as enthalpy change (ΔH), entropy change (ΔS), and free energy change (ΔG). The values of these thermodynamic parameters can be calculated through the following equations:

$$\ln K_a = -\frac{\Delta H}{RT} + \frac{\Delta S}{R} \quad (4)$$

$$\Delta G = \Delta H - T\Delta S \quad (5)$$

As shown in Figure 7F, good linear relationships are existed between $\ln K_a$ and $1/T$ in these ctDNA(AO)–compound systems. The calculated ΔH, ΔS, and ΔG values were all incorporated in Table 1. The negative values of ΔG suggest that the intercalative binding processes of these compounds with ctDNA–AO complex have occurred spontaneously.[40] Moreover, the negative values of both ΔH and ΔS imply that the hydrogen bonds and van der Waals interactions play major roles during their intercalative binding reactions.[40]

3.5 | CD spectrometry

CD spectrometry is an effective technique to investigate the chiral conformation of DNA after its interaction with small molecules. In order to reveal the influence of these compounds on the chiral conformation of ctDNA, CD spectra of compounds, and ctDNA without or with different concentration of compounds were illustrated in Figure 8. It is apparent that all compounds are not optically active and exhibit almost no CD signals in the measuring UV regions. However, ctDNA exhibits an obvious CD spectrum consisted of a negative band at 246 nm due to the right-handed B-form helicity and a positive

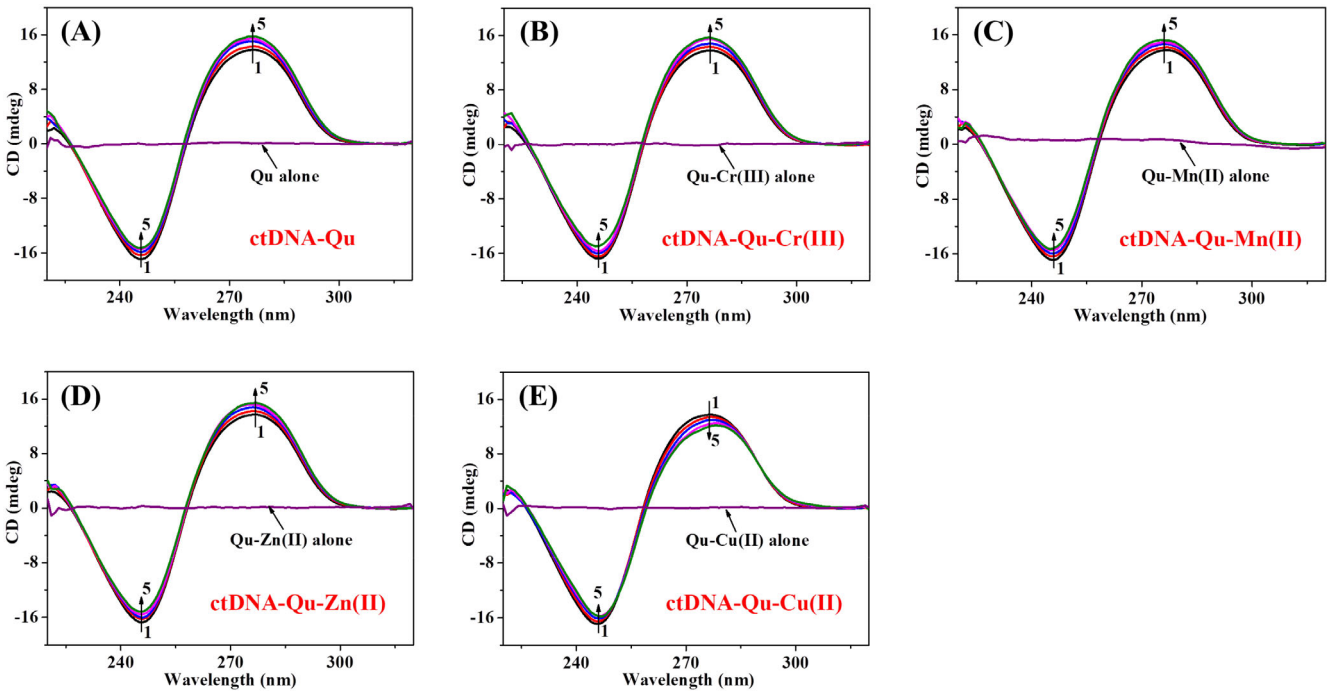

FIGURE 8 A. CD spectra of Qu and ctDNA-Qu systems with different molar ratio of [Qu]/[ctDNA]. B. CD spectra of Qu-Cr(III) and ctDNA-Qu-Cr(III) systems with different molar ratio of [Qu-Cr(III)]/[ctDNA]. C. CD spectra of Qu-Mn(II) and ctDNA-Qu-Mn(II) systems with different molar ratio of [Qu-Mn(II)]/[ctDNA]. D. CD spectra of Qu-Zn(II) and ctDNA-Qu-Zn(II) systems with different molar ratio of [Qu-Zn(II)]/[ctDNA]. E. CD spectra of Qu-Cu(II) and ctDNA-Qu-Cu(II) systems with different molar ratio of [Qu-Cu(II)]/[ctDNA]

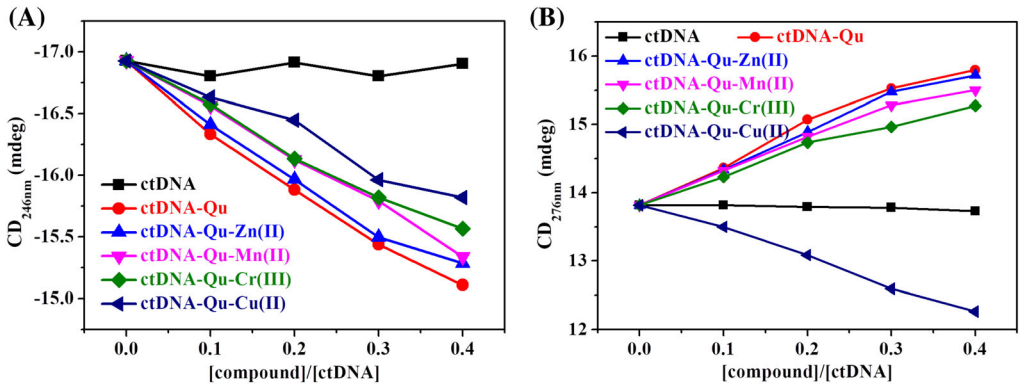

FIGURE 9 A, Curves of CD intensity at 246 nm vs [compound]/[ctDNA]. B, Curves of CD intensity at 276 nm vs [compound]/[ctDNA]

band at 276 nm ascribed to the base pair stacking.[41] Various studies suggest that both absorption bands are quite susceptible to the interaction with small molecules. The intercalative binding of small molecules into the double helical structure of DNA can significantly affect the positive and negative peaks, while DNA interaction with small molecules at the electrostatic interaction and grooves binding only induces less change on the native CD spectrum of DNA.[42] As shown in Figure 8A-D, with the increase of the molar ratio of [compound]/[ctDNA], the intensity of the negative band at 246 nm of ctDNA is decreased significantly but the intensity of the positive band at 276 nm of ctDNA is increased obviously without any remarkable shift in the band position. These changes in CD spectra are attributed to the decrease in the right-handed B-form helicity but the increase in the base pair stacking.[22] Therefore, Qu, Qu–Cr(III), Qu–Mn(II), and Qu–Zn(II) can decrease the right-handed B-form helix structure of ctDNA but increase the base pair stacking of ctDNA. However, with the increase of the concentration of Qu–Cu(II) complex, the intensities of both negative band at 246 nm and positive band at 276 nm are all decreased obviously (Figure 8E). Consequently, Qu–Cu(II) complex can decrease both the right-handed B-form helicity and the base pair stacking of ctDNA. These significant changes of the right-handed B-form helicity and base pair stacking of ctDNA structure are ascribed to the intercalative binding of these compounds with ctDNA. Since Qu–Cu(II) complex decreases the base pair stacking of ctDNA, the double helical structure of ctDNA becomes much loosen, resulting in the lower binding ability of Qu–Cu(II) complex with ctDNA than Qu and other Qu–metal complexes.

As exhibited in Figure 9A, the intensity of negative band at 246 nm is decreased gradually with the continuous addition of these compounds. The decreasing tendency of the intensity of negative band at 246 nm upon the addition of these compounds is in the following order: Qu > Qu–Zn(II) > Qu–Mn(II) > Qu–Cr(III) > Qu–Cu(II). In addition, the increasing tendency of the intensity of positive band at 276 nm from high to low is Qu > Qu–Zn(II) > Qu–Mn(II) > Qu–Cr(III) (Figure 9B). These results indicate that Qu can affect the chiral conformation of ctDNA more significantly than Qu–metal complexes, mainly because of its less space steric hindrance. Among Qu–Zn(II), Qu–Mn(II), and Qu–Cr(III) complexes, Qu–Zn(II) complex can decrease the right-handed B-form helicity but increase the base pair stacking of ctDNA more obviously than other two Qu–metal complexes, while Qu–Cr(III) complex shows the smallest influence on the chiral conformation of ctDNA. Therefore, these Qu–metal complexes can intercalate into the double helical structure of ctDNA and then induce its unwinding but enhance the base pair stacking of ctDNA. However, Qu–Cu(II) complex can not only unwind the double helical structure of ctDNA but also reduce the base pair stacking, resulting in its lowest binding constant among Qu–metal complexes.

4 | CONCLUSIONS

In this work, binding interactions of Qu and Qu–metal complexes with ctDNA were comparatively investigated by UV-vis absorption spectrometry, fluorescence spectrometry, CD spectrometry, viscosity measurement, and DNA melting techniques. These compounds intercalated into the double helical structure of ctDNA and affected the chiral conformation of ctDNA. The fluorescence of ctDNA(AO) complex was quenched by these compounds via static fluorescence quenching mode, and the binding interaction was driven mainly by hydrogen bonds and van der Waals interactions. Among these compounds, Qu–Cr(III) complex interacted with ctDNA more strongly than other compounds, while Qu–Cu(II) complex not only unwound the duplex ctDNA but also reduced its base pair stacking. Therefore, Qu–Cr(III) complex exhibited the strongest binding ability but Qu–Cu(II) complex showed the weakest binding capacity among these Qu–metal complexes. These results make a better understanding of structural influences on the interaction between Qu–metal complexes and ctDNA from molecular biology level, which is very important for the biological applications of these compounds.

ACKNOWLEDGEMENTS

This work was financially supported by National Natural Science Foundation of China (21763005, 21563006, 21864006, 21563010), Natural Science Foundation of Guangxi Province (2017GXNSFDA198034, 2017GXNSFFA198005, 2021GXNSFAA075015), Thousands of Young Teachers Training Program of Guangxi Province (guijiaoren[2018]18), and BAGUI Scholar Program of Guangxi Province of China.

CONFLICT OF INTEREST

The authors declare that they have no known competing financial interests or personal relationships that could have appeared to influence the work reported in this paper.

AUTHOR CONTRIBUTIONS

Huajian Luo and Yu Liang: Performed the research. **Qi Xiao and Shan Huang:** Designed the research study. **Huiying Zhang and Yi Liu:** Contributed essential reagents or tools. **Shan Huang, Huajian Luo, and Yu Liang:** Analyzed the data. **Shan Huang and Huajian Luo:** Wrote the paper.

DATA AVAILABILITY STATEMENT

The data that support the findings of this study are available from the corresponding author upon reasonable request.

ORCID

Qi Xiao https://orcid.org/0000-0002-6133-1853

REFERENCES

1. Osowski A, Kasparek A, Wieczorek Z, Amarowicz R, Szabelski M. Evaluation of the characteristics of some plant polyphenols as molecules intercepting mitoxantrone. *Food Chem*. 2017;227:142-148.
2. Srivastava S, Somasagara RR, Hegde M, et al. Quercetin, a natural flavonoid interacts with DNA, arrests cell cycle and causes tumor regression by activating mitochondrial pathway of apoptosis. *Sci Rep*. 2016;6:24049.
3. Zhu LC, Chen JQ, Tan J, Liu X, Wang BC. Flavonoids from Agrimonia pilosa Ledeb: free radical scavenging and DNA oxidative damage protection activities and analysis of bioactivity-structure relationship based on molecular and electronic structures. *Molecules*. 2017;22:195.
4. Khan F, Niaz K, Maqbool F, et al. Molecular targets underlying the anticancer effects of quercetin: an update. *Nutrients*. 2016;8:529.
5. Abdel-Wahhab MA, Aljawish A, El-Nekeety AA, Abdel-Aziem SH, Hassan NS. Chitosan nanoparticles plus quercetin suppress the oxidative stress, modulate DNA fragmentation and gene expression in the kidney of rats fed ochratoxin A-contaminated diet. *Food Chem Toxicol*. 2017;99:209-221.
6. Sharma DR, Sunkaria A, Wani WY, et al. Quercetin protects against aluminium induced oxidative stress and promotes mitochondrial biogenesis via activation of the PGC-1α signaling pathway. *Neurotoxicology*. 2015;51:116-137.
7. Huang S, Zhu FW, Xiao Q, Liang Y, Zhou Q, Su W. Thermodynamic investigation of the interaction between the [(η^6-p-cymene)Ru(benzaldehyde-N^4-phenylthiosemicarbazone)cl]cl anticancer drug and ctDNA: multispectroscopic and electrochemical studies. *RSC Adv*. 2015;5:42889-42902.
8. Raze A, Xu XQ, Xia L, Xia CK, Tang J, Ouyang Z. Quercetin-iron complex: synthesis, characterization, antioxidant, DNA binding, DNA cleavage, and antibacterial activity studies. *J Fluoresc*. 2016;26:2023-2031.
9. Dolatabadi JEN. Molecular aspects on the interaction of quercetin and its metal complexes with DNA. *Int J Biol Macromol*. 2011;48:227-233.
10. Bukhari SB, Memon S, Mahroof-Tahir M, Bhanger MI. Synthesis, characterization and antioxidant activity copper–quercetin complex. *Spectrochim Acta A*. 2009;71:1901-1906.
11. Zhou J, Wang LF, Wang JY, Tang N. Antioxidative and anti-tumour activities of solid quercetin metal(II) complexes. *Transition Met Chem*. 2001;26:57-63.
12. Tan J, Zhu LC, Wang BC. From GC-rich DNA binding to the repression of survivin gene for quercetin nickel (II) complex: implications for cancer therapy. *Biometals*. 2010;23:1075-1084.
13. Kara HES. Redox mechanism of anticancer drug idarubicin and in-situ evaluation of interaction with DNA using an electrochemical biosensor. *Bioelectrochemistry*. 2014;99:17-23.
14. Campbell NH, Smith DL, Reszka AP, Neidle S, O'Hagan D. Fluorine in medicinal chemistry: β-fluorination of peripheral pyrrolidines attached to acridine ligands affects their interactions with G-quadruplex DNA. *Org Biomol Chem*. 2011;9:1328-1331.
15. Akiyama Y, Ma Q, Edgar E, Laikhter A, Hecht SM. Identification of strong DNA binding motifs for bleomycin. *J Am Chem Soc*. 2008;130:9650-9651.
16. Li XL, Hu YJ, Wang H, Yu BQ, Yue HL. Molecular spectroscopy evidence of berberine binding to DNA: comparative binding and thermodynamic profile of intercalation. *Biomacromolecules*. 2012;13:873-880.
17. Cornard JP, Merlin JC. Spectroscopic and structural study of complexes of quercetin with Al(III). *J Inorg Biochem*. 2002;92:19-27.
18. Coury JE, McFail-Isom L, Williams LD, Bottomley LA. A novel assay for drug-DNA binding mode, affinity, and exclusion number: scanning force microscopy. *Proc Natl Acad Sci U S A*. 1996;93:12283-12286.
19. Tan J, Wang BC, Zhu LC. DNA binding and oxidative DNA damage induced by a quercetin copper(II) complex: potential mechanism of its antitumor properties. *J Biol Inorg Chem*. 2009;14:727-739.
20. Ni YN, Du S, Kokot S. Interaction between quercetin—copper (II) complex and DNA with the use of the Neutral Red dye fluorophor probe. *Anal Chim Acta*. 2007;584:19-27.
21. Tu B, Liu ZJ, Chen ZF, Ouyang Y, Hu YJ. Understanding the structure—activity relationship between quercetin and naringenin: in vitro. *RSC Adv*. 2015;5:106171.
22. Huang S, Liang Y, Huang CS, et al. Systematical investigation of binding interaction between novel ruthenium(II) arene complex with curcumin analogs and ctDNA. *Luminescence*. 2016;31:1384-1394.
23. Martinez R, Chacon-Garcia L. The search of DNA-intercalators as antitumoral drugs: what worked and what did not work. *Curr Med Chem*. 2005;12:127-151.
24. Blackburn GM, Gait MJ. *Nucleic Acids in Chemistry and Biology*. 2nd ed. New York: Oxford University Press; 1996.
25. Kashanian S, Dolatabadi JEN. In vitro study of calf thymus DNA interaction with butylated hydroxyanisole. *DNA Cell Biol*. 2009;28:535-540.
26. Zhou XY, Zhang GW, Wang LH. Binding of 8-methoxypsoralen to DNA in vitro: monitoring by spectroscopic and chemometrics approaches. *J. Lumin*. 2014;154:116-123.
27. Kurbanoglu S, Dogan-Topal B, Hlavata L, Lubuda J, Ozkan SA, Uslu B. Electrochemical investigation of an interaction of the antidepressant drug aripiprazole with original and damaged calf thymus dsDNA. *Electrochim Acta*. 2015;169:233-240.
28. Li Y, Zhang GW, Tao M. Binding properties of herbicide chlorpropham to DNA: spectroscopic, chemometrics and modeling investigations. *J Photochem Photobiol B*. 2014;138:109-117.
29. Dostani M, Kianfar AH, Mahmood WAK, et al. An experimental and theoretical study on the interaction of DNA and BSA with novel Ni^{2+}, Cu^{2+} and VO^{2+} complexes derived from vanillin bidentate Schiff base ligand. *Spectrochim Acta A*. 2017;180:144-153.
30. Shahabadi N, Amiri S. Spectroscopic and computational studies on the interaction of DNA with pregabalin drug. *Spectrochim Acta A*. 2015;138:840-845.
31. Li Y, Zhang GW, Pan JH, Zhang Y. Determination of metolcarb binding to DNA by spectroscopic and chemometrics methods with the use of acridine orange as a probe. *Sens Actuators B: Chem*. 2014;191:464-472.
32. Cohen G, Eisenberg H. Viscosity and sedimentation study of sonicated DNA–proflavine complexes. *Biopolymers*. 1969;8:45-55.

33. Rambabu A, Kumar MP, Tejaswi S, Vamsikrishna N, Shivaraj. DNA interaction, antimicrobial studies of newly synthesized copper (II) complexes with 2-amino-6-(trifluoromethoxy)benzothiazole Schiff base ligands. *J Photochem Photobiol B*. 2016;165:147-156.
34. Asadi Z, Nasrollahi N, Karbalaei-Heidari H, et al. Investigation of the complex structure, comparative DNA-binding and DNA cleavage of two water-soluble mono-nuclear lanthanum(III) complexes and cytotoxic activity of chitosan-coated magnetic nanoparticles as drug delivery for the complexes. *Spectrochim Acta A*. 2017;178:125-135.
35. Kumar CV, Turner RS, Asuncion EH. Groove binding of a styrylcyanine dye to the DNA double helix: the salt effect. *J Photochem Photobiol A*. 1993;74:231-238.
36. Zhang SF, Sun XJ, Kong RM, Xu MM. Studies on the interaction of apigenin with calf thymus DNA by spectroscopic methods. *Spectrochim Acta A*. 2015;136:1666-1670.
37. Dustkami M, Mansouri-Torshizi H. Refolding and unfolding of CT-DNA by newly designed Pd(II) complexes. Their synthesis, characterization and antitumor effects. *Int J Biol Macromol*. 2017;99:319-334.
38. Lakowicz JR. *Principles of Fluorescence Spectroscopy*. 3rd ed. New York: Springer; 2006.
39. Leckband D. Measuring the forces that control protein interactions. *Annu Rev Biophys Biomol Struct*. 2000;29:1-26.
40. Ross DP, Subramanian S. Thermodynamics of protein association reactions: forces contributing to stability. *Biochemistry*. 1981;20:3096-3102.
41. Zhang YL, Zhang X, Fei XC, Wang SL, Gao HW. Binding of bisphenol A and acrylamide to BSA and DNA: insights into the comparative interactions of harmful chemicals with functional biomacromolecules. *J Hazard Mater*. 2010;182:877-885.
42. Qais FA, Abdullah KM, Alam MM, Naseem I, Ahmad I. Interaction of capsaicin with calf thymus DNA: a multi-spectroscopicand molecular modelling study. *Int J Biol Macromol*. 2017;97:392-402.

How to cite this article: Luo H, Liang Y, Zhang H, Liu Y, Xiao Q, Huang S. Comparison on binding interactions of quercetin and its metal complexes with calf thymus DNA by spectroscopic techniques and viscosity measurement. *J Mol Recognit*. 2021;e2933. doi:10.1002/jmr.2933